Database of High-Z Signatures in Cargo

Ron Bentley
Sensor Concepts and Applications, Inc.
Glen Arm, Maryland
rbentley@scainc.biz

***Abstract*— Results from comprehensive testing of two prototype dual-energy (6 and 9 MeV) cargo inspection systems provide large databases of signature information of various high atomic number objects (active interrogation benchmarks) hidden in representative cargos. Test objects were fabricated from lead, tungsten and uranium ranging in size from 75 to 430,000 cm^3. ISO containers were filled with eighteen selected cargos that varied in density and complexity. These databases, collected by the Domestic Nuclear Detection Office Cargo Advanced Automated Radiography System (CAARS) Program, provide a rich source of signature information that can be used to develop automated and user-assist detection algorithms.**

Keywords-component; Inspection systems, automated detection, dual-energy, High-Z signature.

I. Introduction

Fig. 1 is a radiograph with a simulated threat object hidden among automobile engines in a shipping container. The item includes shielding that would make it undetectable to passive gamma-ray detection systems. As a Customs and Border Protection officer, your job is to identify and interdict smuggled items. If the smuggled item is a radiological or nuclear threat that eludes detection, the consequences could be disastrous.

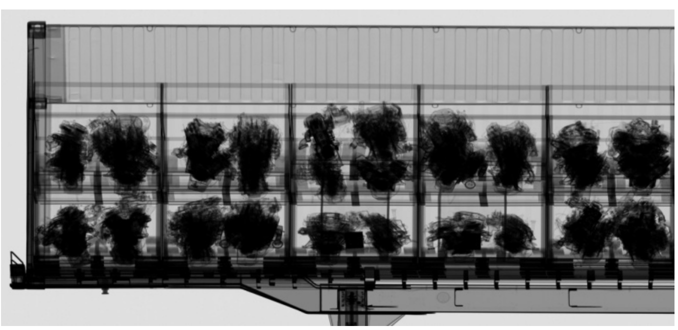

Figure 1. Test object is hidden in cargo container filled with automobile engines.

Inspection systems that rely on human interpretation of radiographs are capacity-limited. On the other hand, routine high-speed inspection of cargo can be performed with x-ray inspection systems that use automated detection algorithms. Algorithms that detect subtle differences between images can thereby relieve inspectors of the tedium that comes with repeated visual interpretation of radiographic images.

Fig. 1 comes from a Domestic Nuclear Detection Office's database of radiographic images collected during test programs. The test programs were conducted to characterize the capabilities of inspection systems that employed dual-energy discrimination.

II. Evolution of Dual Energy Discrimination

In 1975, Alvarez and Maovski advanced the idea of using two x-ray spectra to separate the effects of photoelectric interaction and Compton scattering in order to improve medical diagnostic information extraction from computerized tomography systems [1]. In 1992, Eilbert and Krug described a baggage inspection system based on a single view, dual energy concept [2]. The airport security system was designed to detect explosives and contraband via separation of bag contents based on atomic number. This system's decision software employed "background subtraction" to remove the effects of overlaying objects. In 1996, Neale et al. were granted a patent for an inspection apparatus for subjecting baggage and containers to x-rays of two different energies [3]. Atomic number of the contents was determined from look-up tables based on the ratio of the signals at the two energies. Ogorodnikov and Petrunin extended the idea to a dual energy (4 MeV/ 8 MeV) cargo inspection system useable with full-size shipping containers [4]. With this system, container contents were classified into four atomic number categories: "Organics," "Organics-Inorganics," "Inorganics" and "Heavy Substances."

III. Basis for Dual-Energy Discrimination

Dual-energy discrimination is based on the differences in x-ray attenuation at two separated energies. The difference is best expressed as a ratio of attenuation coefficients. Consider the simple case of a bremsstrahlung source with energy-integrating detectors. Neglecting the interactions within the detector, for:

$N_E(E)$ = number of photons in a pulse directed to the detector (as a function of energy) for spectrum E_E
$\mu_{AIR}(E)$ = attenuation coefficient of air
t_{AIR} = photon travel distance in air

The total single-pulse energy arriving at the detector after travelling through air is:

$$I_{O,E} = \int_0^{E_E} N(E) e^{-\mu_{AIR}(E) t_{AIR}} \, dE. \tag{1}$$

If the path is interrupted by a test object of thickness t with attenuation coefficient μ, the energy at the detector becomes:

$$I_E = \int_0^{E_E} N(E) e^{-\mu_{AIR}(E) t_{AIR}} \, e^{-\mu(E) t} dE. \tag{2}$$

We can define an “average” attenuation coefficient ($\overline{\mu_E}$) for energy spectrum E such that:

$$e^{-\overline{\mu_E}t} = \int_0^{E_E} e^{-\mu(E)t}\, dE. \qquad (3)$$

Then, the natural logarithm of the transmission ratio is:

$$\ln\left({}^{I_E}/_{I_{O,E}}\right) = \ln\left(\frac{\int_0^{E_E} N(E)e^{-\mu_{AIR}(E)t_{AIR}}e^{-\mu(E)t}dE}{\int_0^{E_E} N(E)e^{-\mu_{AIR}(E)t_{AIR}}dE}\right). \qquad (4)$$

Assuming that the effects of the air can be considered independent of the effects of the test object, we have approximately:

$$\ln\left({}^{I_E}/_{I_{O,E}}\right) = -\overline{\mu_E}t. \qquad (5)$$

Taking the ratio of the attenuations at two energies (H = high energy spectrum and L = low energy spectrum) yields:

$$\frac{\ln\left({}^{I_H}/_{I_{O,H}}\right)}{\ln\left({}^{I_L}/_{I_{O.L}}\right)} \cong \frac{\overline{\mu_H}}{\overline{\mu_L}}. \qquad (6)$$

The quantities on the left of (6) are all measurements from the inspection system. The quantity on the right is a property of the test object’s material and is a function of its atomic number. Fig. 2 shows how, in the case of mono-energetic sources, this ratio varies as a function of atomic number. For CAARS, $Z \geq 72$ was considered High-Z.

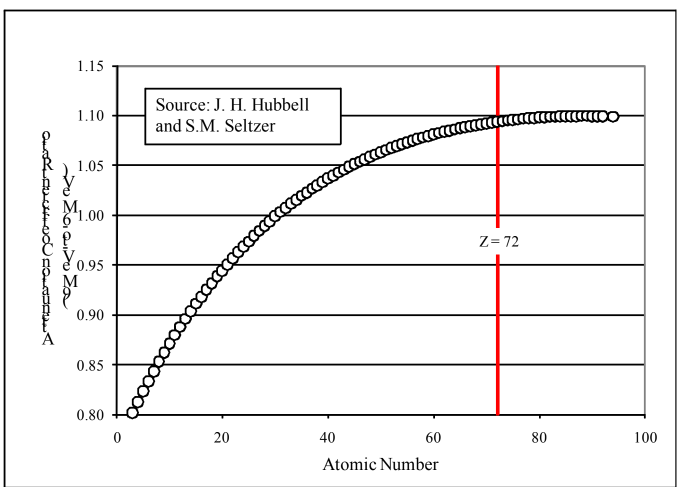

Figure 2. Attenuation ratio is a monotonically increasing function of atomic number.

IV. Overview of DNDO CAARS TD&C

In 2006, DNDO established the Cargo Advanced Automated Radiography System (CAARS) program. Two CAARS prototypes (built by SAIC and L-3) were designed to automatically detect nuclear and shielding material and to enable detection of contraband as well as or better than current systems with minimal impact to port-of-entry operations. The culmination of each program was a government-run test called Technology Demonstration and Characterization (TD&C) conducted in 2009-10.

Three different types of tests were conducted during TD&C but this paper focuses on the Detection-in-Cargo scanning results.

V. Properties of the Prototype CAARS Systems

The two prototype systems are shown in Fig. 3. Each was designed to accommodate a full-size, over-the-road tractor-trailer combination. Both designs were gantries that transported x-ray sources and detector array(s) past a stationery vehicle at a nominal scan rate of 2.7 feet/second. A significant design difference was that the SAIC source was an interlaced accelerator that alternately outputted pulses with peak energies of 6 MeV and 9 MeV. In contrast, the L-3 prototype included two separate accelerators each with its own dedicated detector array.

The CAARS systems were required to detect a 100 cm^3 cube of High-Z material behind 25.4-cm of steel anywhere in the container volume. The false alarm rate was not to exceed 3 occurrences per 100 scans. To meet these requirements, each prototype contained sophisticated software for image processing and automated detection. The systems presented radiographs and other information at the operator’s workstation. When detection occurred, the suspect area was highlighted in one of two ways:

Threat Alarm – Alert provided to operator that there was high confidence that High-Z material was present at the indicated location

Unknown Alarm – Alert provided to the operator that there was insufficient information to make a high confidence decision about the presence of High-Z material at the indicated location.

Figure 3. CAARS prototypes (top: SAIC, bottom: L-3)

VI. Cargo Characteristics

Based on a DHS study of actual cargo densities and complexities, a subset of 18 cargos was selected to represent approximately 70 percent of the most commonly encountered cargo types [6]. The 18 cargos were classified based on two attributes, density and complexity, and organized into these four groups: (1) low density - low complexity; (2) high density - low complexity; (3) low density - high complexity; and (4) high density - high complexity. As shown in Table I, the 18 cargos provided five cargos for three of the four combinations of density and complexity, with the exception that only three cargos made up the low density-low complexity combination.

TABLE I. Classification of 18 cargos used for TD&C.

Cargo Description	Average Pallet Density (g/cm^3)	Density Class	Complexity Class
Denim	0.18		
Tee Shirts	0.17	Low	Low
Toys	0.07		
Tires	0.14		
Metal Furniture	0.12		
TVs	0.16	Low	High
Tools	0.27		
Office Furniture	0.23		
Cement	1.14		
Plastic Scrap	0.36		
Lumber	0.42	High	Low
Newsprint	0.46		
Bottled Water	0.47		
Machine Buckets	0.49		
Transmissions	0.39		
Air Conditioner Parts	0.38	High	High
Brake Parts	0.36		
Engines	0.36		

VII. Test Object Characteristics

Test objects ranged from simple geometric shapes such as cubes and spheres (on the order of 100-400 cm^3) to larger, more complex geometries that possessed properties of interest. The largest of the test objects weighed nearly 1,000 kilograms. Though most test objects were made from High-Z materials (lead, tungsten and uranium), for comparison purposes, some were fabricated from tin and steel. Fig. 4 shows a representative test object ("ball in a box"), which consisted of a central depleted uranium sphere surrounded by a lead-lined steel box. Fig. 4 shows a radiograph of this object along with a false color map of the ratio of attenuations for the two energy spectra.

Figure 4. Representative test object consisted of uranium sphere in a lead box

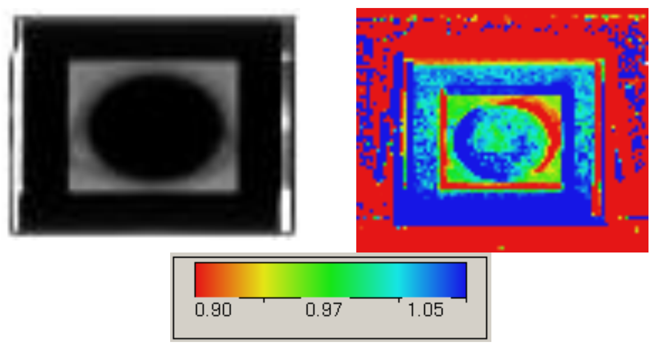

Figure 5. Gray-scale radiograph (left) shows test object details and false-color ratio image (right) is indicative of atomic number (scale at bottom).

Multiple test objects were hidden in the containers. An opportunity for detection of a test object was a "trial." Typically, a container was scanned 12 times and then oriented in the opposite direction for another 12 scans. Table II lists the number of trials in each test TD&C program.

TABLE II. Scope of Detection-in-Cargo Tests

Prototype System	Number of Detection-in-Cargo Trials
SAIC	8,320
L-3	8,312

VIII. Effects of Cargo

The images in Fig. 6 and Fig. 7 demonstrate the effects of cargo on a test object's signature. When placed in a uniform low-density cargo, the test object is readily discernable. Fig. 5 shows the test object in boxed T-shirts. Comparison of values in the ratio image demonstrates the distinctive signature of High-Z materials.

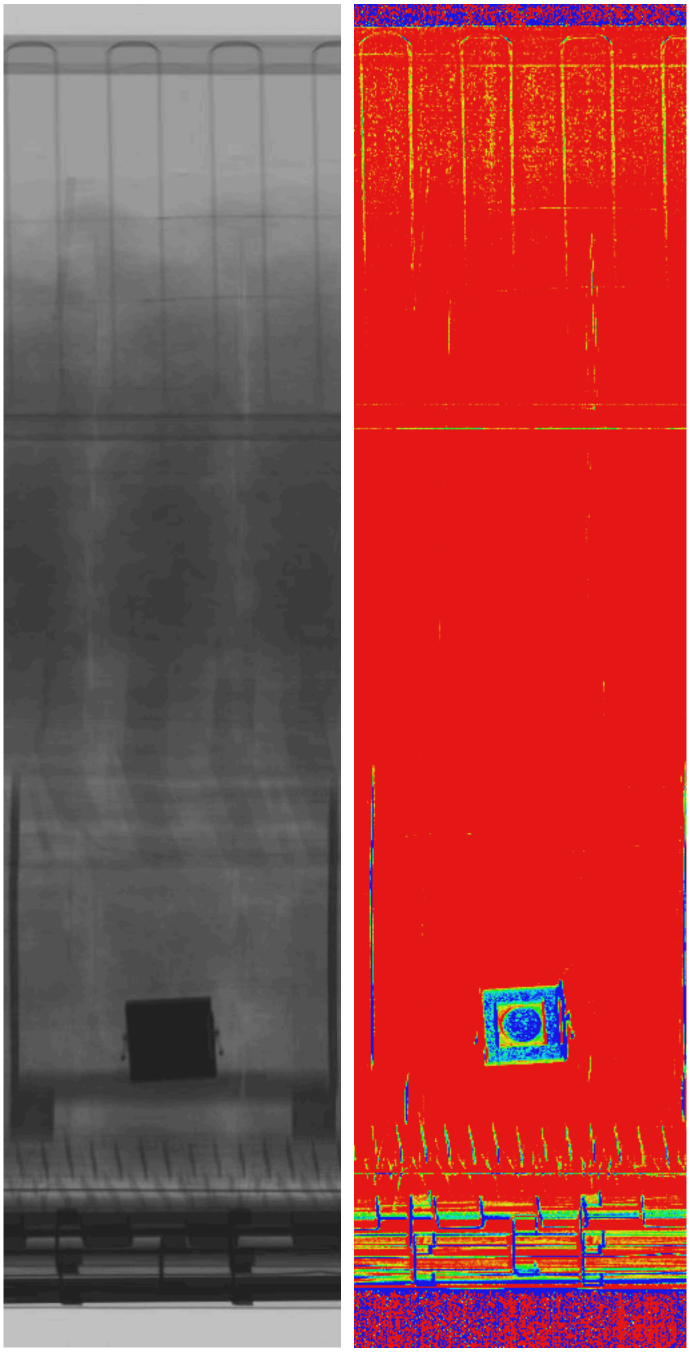

Figure 6. The test object is easily distinguished in both types of images of boxed T-shirts on pallets.

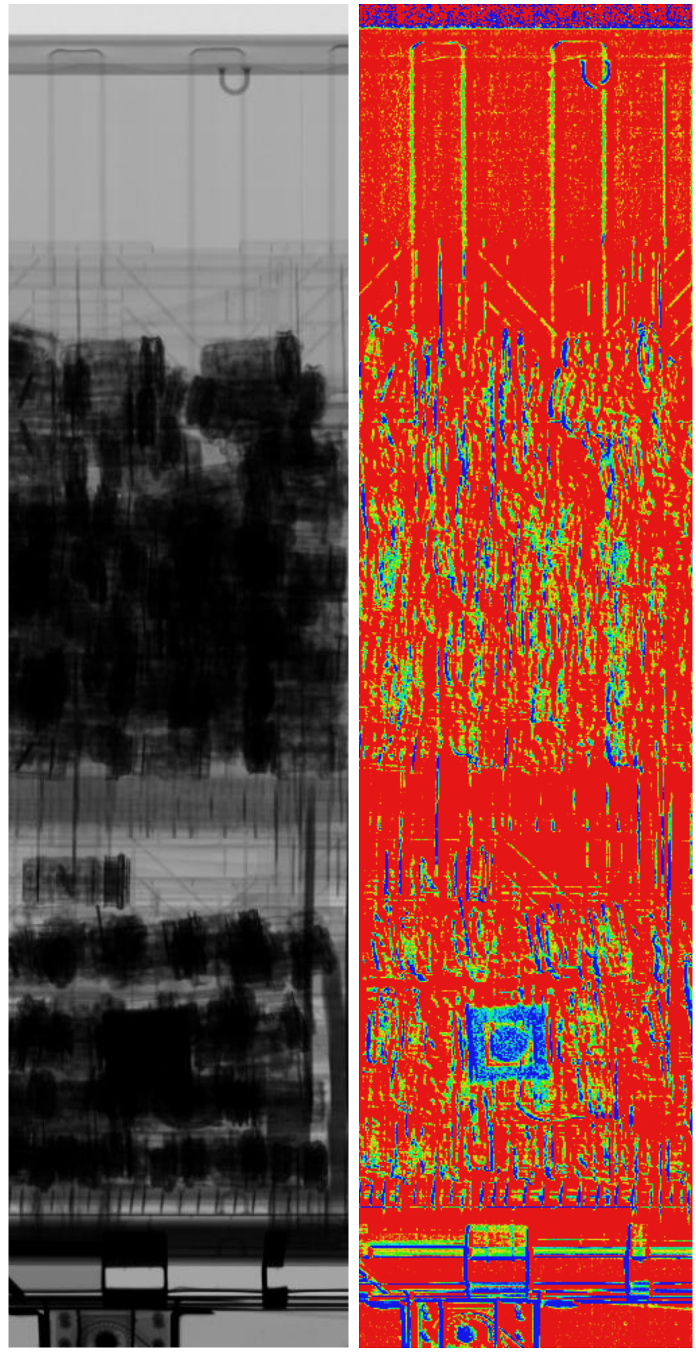

Figure 7. When placed among air compressors of roughly the same size, the test object is difficult to discern in the gray-scale radiograph.

When the density and inhomogenity of the cargo increases, the test object becomes much more difficult to discern. Fig. 7 shows the same test object in automobile air compressor parts of roughly the same size. Even with the cluttering effects of multiple objects, the ratio image provides a signature of high-Z material.

Returning to the image of Fig. 1, Fig.8 shows a close-up of a pallet of engines. The test object is well-hidden in the radiograph , but its signature is apparent in the ratio image.

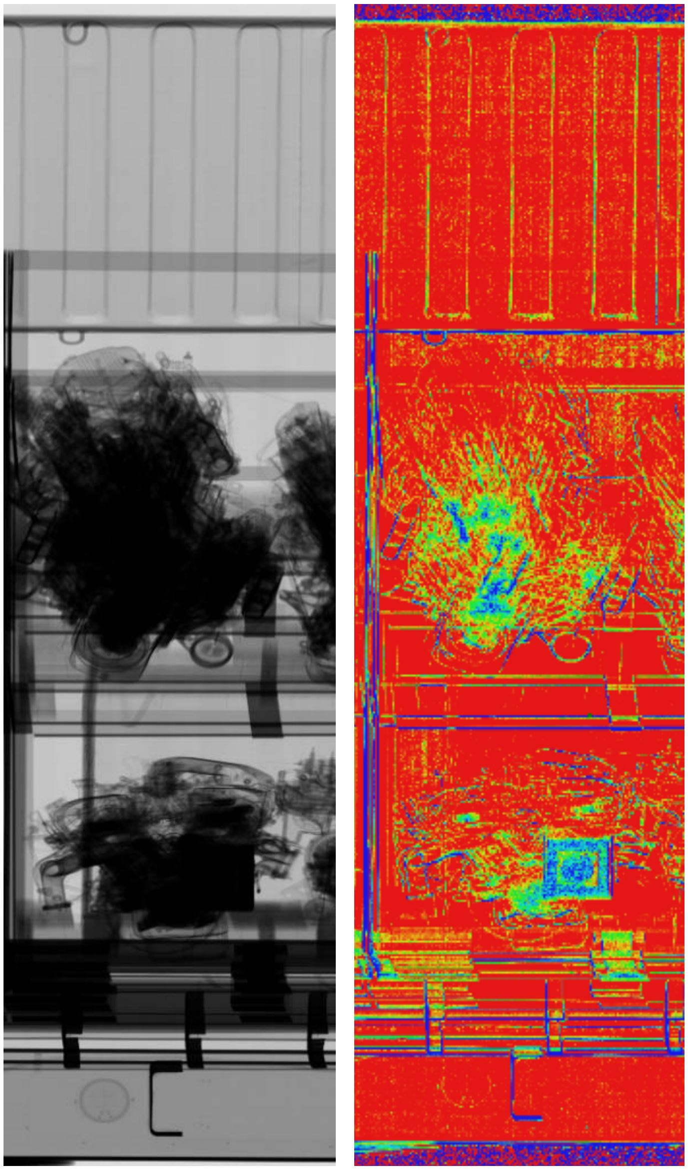

Figure 8. Attenuation coefficient ratio reveals location of test object from Fig. 1.

IX. Use of the Databases

The author's personal experience with the databases has focused on understanding how signal properties affect the ability to generate automated alarms. In addition to the databases for the two dual energy systems, a comparable data base exists for a single energy (6 MeV) inspection system. Besides the vendors who built the x-ray inspection systems, several independent developers have used portions of the databases to explore the capabilities of their unique algorithm approaches.

References

[1] R E Alvarez and A Macovski, "Energy selective reconstructions in X-ray computerized tomography", Phys. Med. Biol, vol 21, pp 733-744, 1976.

[2] R. Eilbert and K. Krug, "Aspects of image recognition in vivid technology's dual-energy X-ray system for explosive detection", in Proc. of SPIE, vol. 1824, 1992.

[3] W.W. Neale, J.G. Rushbrooke and R.E. Ansorge, "Material identification using X-rays," U.S. Patent 5 524 133, June 4, 1996.

[4] S. Ogorodnikov and V. Petrunin, "Processing of interlaced images in 4–10 MeV dual energy customs system for material recognition", Phys. Rev. Accels and Beams, vol. 5, (104701), 2002.

[5] J. H. Hubbell and S.M. Seltzer. *Tables of X-Ray Mass Attenuation Coefficients and Mass Energy-Absorption Coefficients from 1 keV to 20 MeV for Elements Z = 1 to 92 and 48 Additional Substances of Dosimetric Interest*, [Online]. Available: http://www.nist.gov/pml/data/xraycoef/index.cfm

[6] "Standard Cargo for Testing Large-Scale Non-Intrusive Inspection Systems," Domestic Nuclear Detection Office, Washington, D.C., 500-JINII-108620v1.00, December 5, 2008.

ABOUT THE AUTHOR

Ron Bentley is a senior technologist with Sensor Concepts and Applications, Inc. working under contract to the Domestic Nuclear Detection Office within the Department of Homeland Security. Having worked previously for General Dynamics and the US Navy, he has over forty years of experience with complex defense systems. Currently, his professional focus is on the automated detection of nuclear threats with cargo inspection systems. He can be reached at: rbentley@scainc.biz.
